

<sup>1</sup> Transition of eruptive style: pumice raft to dome-forming  
<sup>2</sup> eruption at the Havre submarine volcano

<sup>3</sup> Michael Manga<sup>1</sup>, Samuel J. Mitchell<sup>2</sup>, Wim Degruyter<sup>3</sup>, and Rebecca J. Carey<sup>4</sup>

<sup>4</sup> Department of Earth and Planetary Science, University of California, Berkeley,  
CA 94720, USA

<sup>6</sup> Department of Geology and Geophysics, University of Hawai'i at Manoa,  
Honolulu, HI 96822, USA

<sup>8</sup> School of Earth and Ocean Sciences, Cardiff University, Cardiff CF10 3AT, Wales,  
UK

<sup>10</sup> School of Earth Sciences, University of Tasmania, Hobart, Tasmania 7001,  
Australia

<sup>12</sup> October 30, 2018

<sup>13</sup> **1 Supplementary materials**

Table DR1: Composition and vesicularity of raft and dome OP samples. Composition of raft from Rotella et al. (2015) and dome OP is the average of two values from Carey et al. (2018). Dome OP vesicularity is from Table DR2 and the raft value is mean from Rotella et al. (2015) and Carey et al. (2018).

	raft	dome OP
SiO <sub>2</sub>	72.11	72.20
TiO <sub>2</sub>	0.46	0.46
Al <sub>2</sub> O <sub>3</sub>	13.99	14.11
Fe <sub>2</sub> O <sub>3</sub>	3.35	3.25
MnO	0.12	0.10
MgO	0.64	0.70
CaO	2.67	2.56
Na <sub>2</sub> O	5.15	5.14
K <sub>2</sub> O	1.44	1.40
P <sub>2</sub> O <sub>5</sub>	0.08	0.08
LOI	1.08	0.50
vesicularity	78%	39%

Table DR2: Clast densities measured using the methods of Houghton and Wilson (1989). Vesicularity calculated using a dense rock equivalent density of 2380 kg/m<sup>3</sup>.

sample	unit	fragment mass (g)	density (kg m <sup>-3</sup> )	Vesicularity (%)
HVR0013	Dome P carapace	28.28	1898	20.9
		5.94	1967	18.0
HVR0010	Dome O carapace	11.94	1675	30.2
		8.39	1892	20.5
		5.38	1622	31.8
		2.07	1899	20.9
HVR0007	Dome OP talus	21.64	1384	42.3
		15.22	1407	41.4
		14.22	1365	43.1
		7.02	1390	42.1
		6.46	1366	43.1
		5.46	1362	43.3
		5.17	1249	50.7
		4.92	1348	43.8
		4.63	1272	49.3
		4.27	1400	41.7
		3.58	1253	49.9
		3.40	1429	40.5
		3.27	1422	40.8
		2.21	1348	43.9
		1.46	1446	39.8
		1.45	1394	41.9
		1.43	1444	39.8
		1.37	1370	42.9
HVR0118	Dome OP talus	1.36	1360	43.3
		1.31	1456	39.4
		1.18	1372	42.8
		1.01	1312	45.3
		0.76	1407	41.4
		45.22	1108	53.8
		4.98	1634	31.3
HVR0187	Dome OP talus	4.40	1701	28.5
		60.31	1310	45.4
		14.20	1538	35.9
		8.01	1288	46.3
		2.06	1856	22.7

Houghton B.F. and Wilson C.J.N., 1989, A vesicularity index for pyroclastic deposits:  
 Bulletin of volcanology, v. 51, p. 451-462.

Table DR3: H<sub>2</sub>O concentrations, with two standard deviation error, of melt inclusions within Quartz and Plagioclase. Phenocrysts were taken from raft pumice (RPAUS and RPFJ) and giant pumice (GP). Concentrations acquired through SIMS analysis at the Woods Hole Oceanographic Institution.

Melt inclusion	H <sub>2</sub> O (wt %)	two sigma
RPAUS-F 156	4.63	0.48
RPAUS-F 157	4.58	0.46
RPAUS-C 162	4.32	0.44
RPAUS-K 167	4.47	0.45
RPAUS-A 173	4.66	0.47
RPAUS-H 175	4.94	0.50
RPAUS-C 163	4.46	0.51
RPAUS-C 164	4.45	0.45
RPAUS-L 170	5.59	0.65
RPAUS-A 172	4.99	0.51
RPAUS-L 171	4.82	0.49
RPFJ-F 242	5.04	0.51
RPFJ-F 243	4.97	0.50
RPFJ-D 250	4.28	0.44
RPFJ-R 252	5.10	0.51
RPFJ-E 253	4.99	0.55
RPFJ-O 234	4.78	0.48
RPFJ-O 235	4.90	0.50
RPFJ-I 238	5.20	0.52
RPFJ-Q 240	5.71	0.60
RPFJ-F 241	5.00	0.51
RPFJ-F 245	5.20	0.53
RPFJ-S 254	5.22	0.53
RPFJ-S 255	4.01	0.40
RPFJ-K 236	4.41	0.44
RPFJ-R 251	4.97	0.50
GP-A 188	4.82	0.48
GP-H 204	4.68	0.47
GP-K 210	4.80	0.48
GP-G 214	4.01	0.40
GP-G 215	4.89	0.50
GP-B 187	5.62	0.56
GP-A 190	5.47	0.56
GP-A 192	4.61	0.46
GP-J 194	4.65	0.46
GP-H 203	5.00	0.50
GP-G 213	5.20	0.52
GP-D 201	5.03	0.52
GP-D 202	5.09	0.52
average	4.86	0.80

Table DR4: Variables, parameters and values

variable or parameter	symbol	value	reference
mass flux	$q$	$10^2 - 10^7 \text{ kg/s}$	
lateral gas loss	$Q_w$	calculated	equation (8)
conduit radius	$r$	12 and 30 m	
depth below seafloor	$z$	0 – 5000 m	
vent depth		900 m	
exsolved gas volume fraction	$\phi$	calculated	
melt velocity	$u_l$	calculated	
gas velocity	$u_g$	calculated	
pressure	$P$	calculated	
temperature	$T$	850°C	Manga et al. (2018)
chamber pressure	$P_{ch}$	calculated	
dissolved gas mass fraction	$c$	calculated	equation (5)
initial gas mass fraction	$c_0$	4.9 weight %	Table DR3
saturation constant	$s$	$4.11 \times 10^{-6} \text{ Pa}^{-1/2}$	
melt density	$\rho_l$	$2400 \text{ kg/m}^3$	Manga et al. (2018)
gas density	$\rho_g$	calculated	
country rock density	$\rho_r$	$2400 \text{ kg/m}^3$	
gas viscosity	$\mu_g$	$10^{-5} \text{ Pa s}$	
melt viscosity	$\mu_l$	calculated	Giordano et al. (2008)
magma viscosity	$\mu_m$	calculated	Llewellyn and Manga (2005)
magma permeability	$k$	calculated	Mueller et al. (2005)
wall rock permeability	$k_w$	$10^{-14} - 10^{-12} \text{ m}^2$	
magma-wall drag	$F_{lw}$	calculated	equation (6)
gas-melt drag	$F_{lg}$	calculated	equation (7)

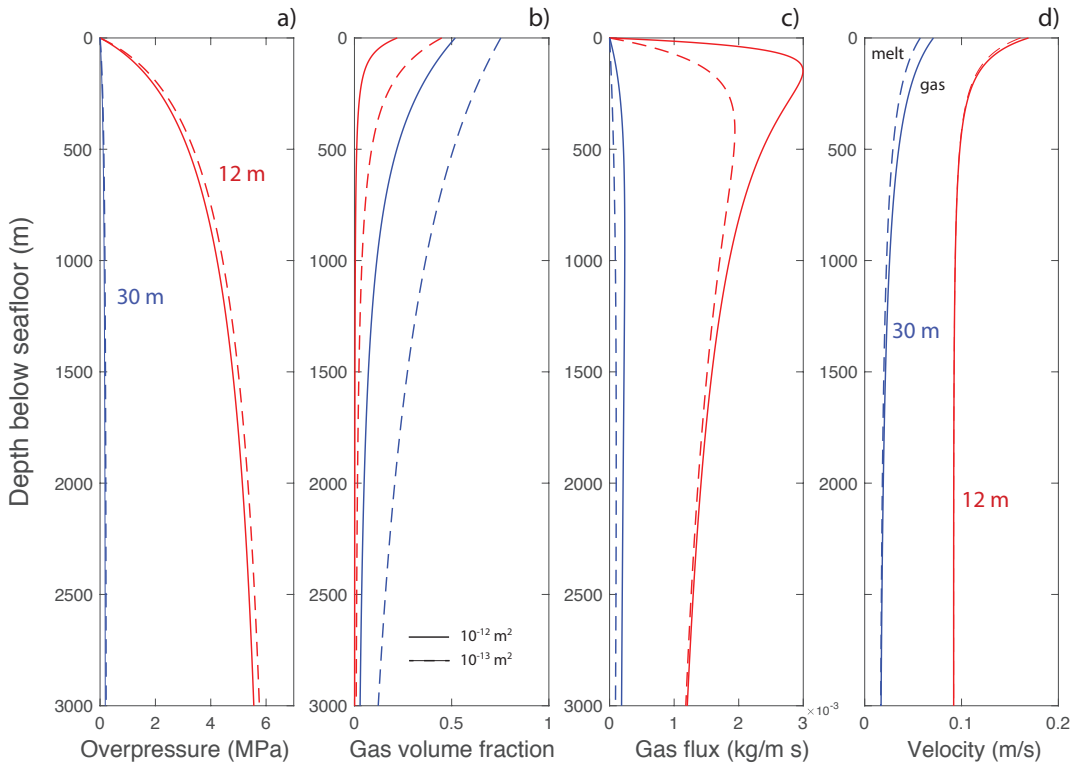


Figure DR5. a) Overpressure (magma pressure minus country rock pressure) and b) vesicularity, and c) volatile flux through the conduit walls (mass per unit height per unit time), as a function of depth for a representative mass eruption rate of  $10^5 \text{ kg/s}$  and two different conduit radii (12 and 30 m) and country rock permeabilities ( $10^{-12}$  and  $10^{-13} \text{ m}^2$ ). d) Gas (solid curves) and melt (dashed curves) ascent velocity for the same mass eruption rate and  $k_w = 10^{-13} \text{ m}^2$ .